

DESIGN AND AERODYNAMIC OPTIMIZATION OF A THIN-HAUL AIRCRAFT WITH DISTRIBUTED ELECTRIC PROPULSION: ZETHA

Giacomo Beghetto¹ & Maurizio Boffadossi¹

¹Dipartimento di Scienze e Tecnologie Aerospaziali, Politecnico di Milano, Via La Masa 34, 20156 Milano

Abstract

This paper presents a comprehensive study on the design and aerodynamic optimization of a fully electric thin-haul aircraft equipped with the innovative Distributed Electric Propulsion (DEP) technology. The research focuses on various crucial aspects, commencing with the Conceptual and Preliminary Design phases, which entail a thorough evaluation of the aircraft's performance parameters, ensuring compliance with rigorous flight mechanics requirements and achieving the performance set during the Pre-Conceptual Design. Subsequently, an initial structural sizing was performed for the purpose of preliminarily define the aircraft's masses through a load-based sizing approach based on the certification category. Aerodynamic optimization of the wing airfoil was pursued to enhance the aircraft's operational range and efficiency. It consists of a detailed investigation into the optimal airfoil performance, setting multiple weighted parameters to be optimized, with the aim of obtaining a high-performing airfoil for various flight phases, characterized by both high lift coefficient values and notable efficiency during the cruise phase. The obtained airfoil was studied using CFD to analyze its high-lift capabilities, both in a clean configuration and with the addition of a Fowler flap. Thus, the study addresses the influence of DEP propellers on the aircraft's wing. The interaction between the DEP system and the aerodynamic characteristics of the wing was analyzed, considering factors such as thrust distribution, flow patterns, and overall lift enhancement. In particular, it was approached by analyzing, using a low-fidelity method, the effects on the wing of the DEP considering a variable number of propellers. Subsequently, a mid-fidelity study was conducted, considering a single propeller and a wing section as a case study to obtain the optimal configuration in terms of lift coefficient enhancement. Overall, this research contributes to the advancement of electric aviation technology, offering valuable insights into the design and optimization of fully electric thin-haul aircraft with the innovative DEP system. The results presented are expected to lay the groundwork for additional further analyses and advancements aimed to DEP implementation.

Keywords: Distributed Electric Propulsion, Thin-Haul, Aerodynamic Optimization, Multifidelity Aerodynamic Analysis, Lift Enhancement

1. Introduction

1.1 General Overview

The need for transportation means characterized by speed and environmental sustainability is a central theme in the development of this work. In fact, in recent years, a strong demand for innovative aircraft, which exploit the concept of On-Demand Mobility and are characterized by high efficiency, as well as low emissions, has been recently highlighted by NASA along with European institutions. Thin-haul commuters can bridge this market gap. These regional 7-9 passenger aircraft directly connect small cities in a point-to-point manner, offering dynamic scheduling for aviation services. These concepts leverage cutting-edge technologies, including electric propulsion and advanced power management systems, combined with state-of-the-art aerodynamics, to extend the operational mission range while simultaneously drastically reducing energy consumption and controlling operating costs. The most pronounced advantages are observed in regions characterized by underdeveloped high-speed rail networks, as is the case in a majority of the U.S., and in areas where road transport is

hindered by rugged terrain, as in central Europe. Thus, there are many operational areas where using thin-haul aircraft is the practical choice due to their efficiency, speed, and environmental impact.

1.2 ZETHA

In light of the considered needs, the design of a full-electric thin-haul aircraft with Distributed Electric Propulsion (DEP) for the On-Demand Mobility of 7 passengers has been developed. This Zero Emission Thin-Haul Aircraft (ZETHA) is intended to cover approximately $400\,km$ in no more than $80\,$ minutes, at a cruising speed of $100\,m/s$.

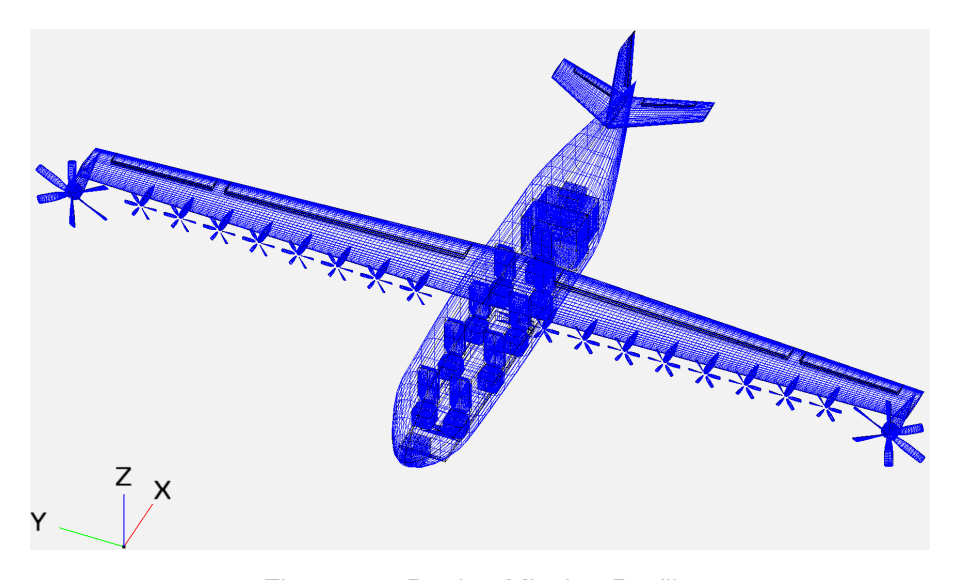


Figure 1 – Design Mission Profile.

The design flow began with a Pre-Conceptual Design phase, followed by a Conceptual phase, and finally a Preliminary Design. Subsequently, the aerodynamic aspects of the project were further explored using a two-dimensional approach, addressing the aerodynamic optimization of the airfoil and designing and studying the related Fowler flap. Next, the three-dimensional aerodynamics of the wing were addressed, analyzing both the effects of the high-lift devices and the contribution to lift enhancement due to DEP. A sensitivity analysis was conducted to identify the best configuration in terms of lift increase due to the DEP propellers' slipstream, evaluating the interference effects leading to thrust degradation.

2. Design

2.1 Pre-Conceptual Design and Innovative Technologies

The initial step of the Pre-Conceptual analysis involved a market analysis aimed at defining the mission profile and the payload characterizing the aircraft. The research findings on thin-hauls projected 81 million trips by 2030, accounting for 6% of the market share. Additionally, thin-hauls are expected to reduce direct operating costs by approximately 20%, primarily due to a significant decrease in energy costs (approximately 71%), as reported in [1]. Consequently, the design range was set at $400\,km$, and the payload of ZETHA was established at $830\,kg$, considering 7 passengers weighing $77\,kg$ each, along with $15\,kg$ of baggage per passenger. The thin-haul accommodates 2 pilots, with their associated masses considered in a similar manner as for passengers. The maximum allowable aircraft weight has been capped at $5440\,kg$ in compliance with regulations (FAR 23 category). The image 2 depicts the design mission profile.

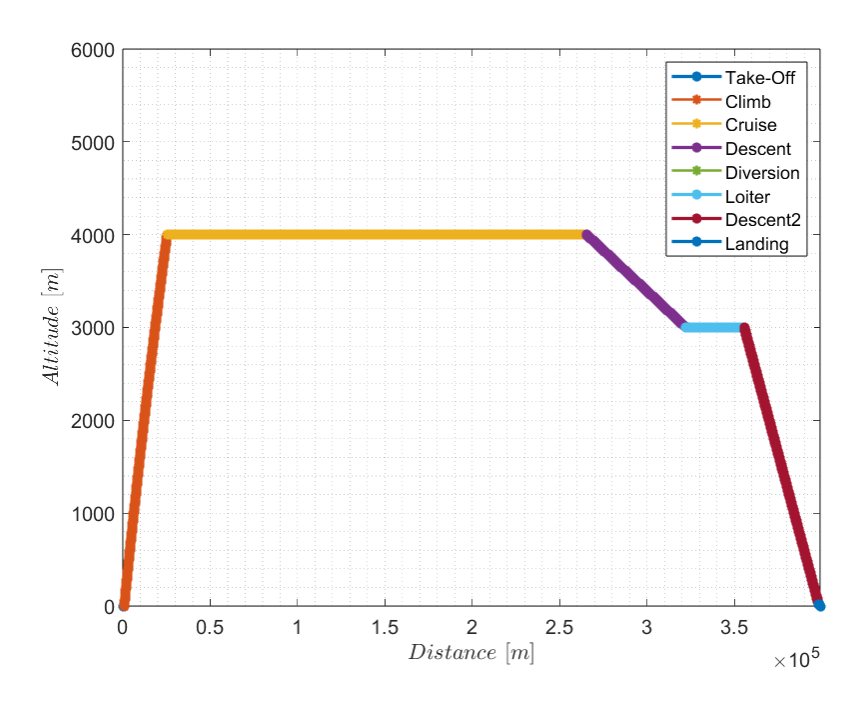


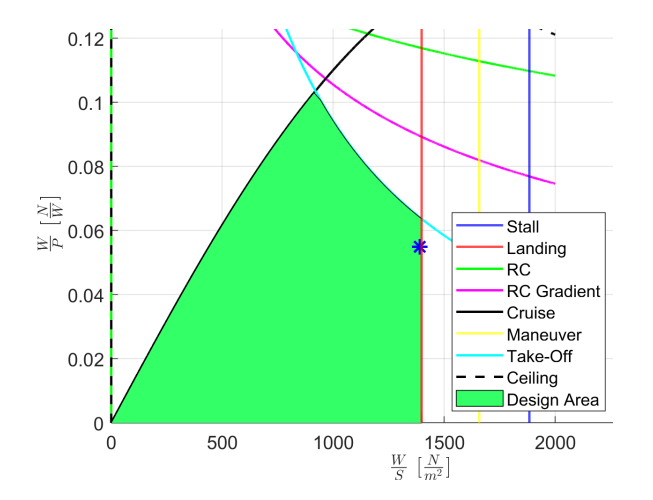
Figure 2 – Design Mission Profile.

The utilization of DEP necessitated an in-depth examination: the interaction between propulsion and aerodynamics enabled by DEP leads to important improvements that have to be considered for the overall wing design. The main effect to be highlighted results to be the enhancement of the lift coefficient C_L , later analyzed. The increase of the lift coefficient is expected to be about 20-30% in clean configuration and of about 50% in flapped configuration, with respect to the wing with DEP deactivated [6]. It is due to the higher local velocity experienced by the wing sections hit by the flow accelerated by the propellers and to the higher angle of attack induced by the upward blade. A thorough investigation has been conducted on the battery to be used and on the arrangement of cells to form battery packs. The research for the battery to be used for this application was conducted by evaluating batteries from an energy perspective, such as Li-Po batteries, characterized by limited energy density, Li-Ion batteries, which have limited power density, and the Lithium-Sulfur (Li-S) cells, which are the most promising contenders within the next 5-10 years both in terms of specific energy and density [3]. The expected advancements hold substantial promise for addressing the specific energy density requirements crucial for the thin-haul category, up to $550-600 \, \frac{Wh}{kg}$. Moreover, a different approach has been considered, evaluating the structural all-solid-state supercapacitors, which are not meant to replace the typical battery pack, as the latter is limited in terms of stored energy. Therefore, a combination of the two systems would be the solution. Nevertheless, after analyzing the power demand of the aircraft, Li-S cells were chosen. In particular, a prototype produced by Sion Power, which is characterised by a specific energy of $350 \frac{Wh}{kg}$ and a specific power of $1340 \frac{W}{kg}$.

2.2 Conceptual Design

The aim of the Conceptual Design phase is to assess the technical feasibility of the full-electric thin-haul. The quantities that have to be defined are the macroscopic ones: the maximum take-off weight (MTOW), the wing surface (S), the power (P) or the thrust (T) installed depending on the type of propulsive system installed, the power loading $\frac{W}{P_b}$ and wing loading $\frac{W}{S}$. Regarding aerodynamics, some targets on the coefficients must be set for the crucial flight phases in order to guarantee the feasibility of the mission from a performance point of view. In order to draft the sizing matrix plot, the aerodynamics of the aircraft must be estimated by means of an analytical or parabolic polar, $C_D = C_{D0} + kC_L^2$, where C_{D0} is the zero-lift drag coefficient and k is a parameter related to the Oswald factor e, defined as $k = \frac{1}{\pi \cdot AR \cdot e}$. Both C_{D0} and e can be retrieved using a statistical approach, following common aircraft design books, such as Roskam [2]. Moreover, it is necessary to consider three different polars (and relative coefficients C_{D0} , k) for clean, take-off, and landing configuration, to correctly ensure the

constraints of the sizing matrix plot. To build the parabolic polar of the aircraft, it is necessary to guess some of the geometric characteristics of the wing and the fuselage. The process adopted to define the sizing matrix plot is iterative and convergence is achieved when the aspect ratio of the wing AR stabilizes within a certain tolerance from one iteration to another. At each step, the wingspan b and the aspect ratio of the wing AR are fixed, and subsequently both C_{D0} and k are computed. Once the aerodynamics are characterised, the mission constraints are imposed for the following flight conditions: take-off, landing, stall, maneuver, rate of climb, rate of climb gradient, cruise, and service ceiling. Therefore both the wing loading $\frac{W}{S}$ and the power loading $\frac{W}{P_b}$ are obtained and the convergence is checked.



$\frac{W}{S}$	$1406 \frac{N}{m^2}$
$\frac{W}{P_b}$	$55 \frac{N}{kW}$
MTOW	3930 kg
S	$27.4 m^2$
P_b	700 kW

Table 1 – Results of the sizing matrix plot.

Figure 3 – Sizing matrix plot.

In order to enhance the performance provided by the Distributed Electric Propulsion, it has been decided to divide the propulsion system into two different subsystems since the very initial phase of the project. The first is designed to provide sufficient thrust in cruise phase, the second feeds the Distributed Electric Propulsion, made by several small propellers driven by a set of electric motors distributed along the wingspan. To enhance the aerodynamic characteristics of the airplane, it has been decided to consider a high aspect ratio wing, in order to reduce induced drag as much as possible. Another design criterion has been to reduce the wingtip vortices, thus the two large cruise propellers have been positioned on the wingtips. For this reason a high wing configuration has been considered, in order to ensure sufficient clearance when the aircraft is on the ground.

2.3 Preliminary Design

A preliminary design loop has been created in *MATLAB*, involving different disciplines: aerodynamics (on which a particular focus has been set on), flight mechanics, propulsion, structures. The design process has been set up with the following logics:

- sizing and design of the horizontal and vertical tail;
- mass estimation of the aircraft's components;
- analysis of the flight profile and sizing of the battery package;
- estimation of the total mass of the aircraft and the position of the centre of gravity;
- analysis of the static stability, following the two surface formulation and imposing a static margin being between 5% to 15%.

The iterative loop is repeated until the difference between the total mass of the airplane computed at two different iterations has turned lower than a certain threshold. Thus, a parabolic approximation of the aircraft polar has been used, retrieving C_{D0} through a flat plate analogy and including different Form Factors F_F , as seen in the following equations 1, where N_a components (wing, tails or fuselage) are considered, D_{eq} is the equivalent diameter and $\frac{t}{c}$ the relative thickness of the airfoil.

$$\begin{cases} C_{D0} = \sum_{i=1}^{N_a} \frac{C_{Fi} S_{weti} F_{Fi}}{S_{ref}} \\ C_{Fi} = \frac{0.455}{((log_{10}(Re_i))^{2.58} (1 + 0.144Ma^2)^{0.65})} \\ F_{Fwing} = 1 + 2.7 \left(\frac{t}{c}\right)_{max} + 100 \left(\frac{t}{c}\right)_{max}^{4} \\ F_{Ffuselage} = 1 + \frac{60}{\left(\frac{L}{D_{eq}}\right)^{3}} + 0.0025 \left(\frac{L}{D_{eq}}\right) \end{cases}$$

$$(1)$$

Follows a power analysis to size the propulsive system and in particular the battery package: given the flight profile and the parabolic polar of the airplane, the power required at each instant of the mission, and then the total energy, have been obtained describing the different flight conditions with the relative equations.

$$P_{b,TO} = 700 \, kW$$
, $P_{b,climb} = 560 \, kW$
 $P_{b,cr} = 281 \, kW$, $P_{b,LND} = 700 \, kW$

Therefore, the power required to the battery package is retrieved considering the most power demanding condition and the efficiencies associated to the propulsion η_p , the transmission η_{tr} , and the electric motors η_m :

$$P_{bat} = \frac{P_{req}}{\eta_p \eta_{tr} \eta_m} = \frac{P_b}{\eta_{tr} \eta_m} \tag{2}$$

The number of batteries to be connected in series and in parallel has been sized with the same formulation presented by Zhao in [7]. The battery pack has been divided into two different packs: the first one is primarily related to powering the DEP propellers, playing a more critical role in phases that require a higher power input, such as take-off and climb, while the second battery pack is dedicated to providing energy for the cruise phase. Therefore, the sizing formulas for the number of cells in parallel vary depending on the battery pack's function: the battery pack dedicated to powering the DEP has been sized using the Required Power Sizing Method, while the battery pack dedicated to cruising has been sized using the Required Endurance Sizing Method.

At this stage, the DEP and cruise propellers have been introduced. The latter are 2-meter diameter propellers ($P_b = 140.5 \, kW$ each), which operate at $1366 \, RPM$, corresponding to a tip velocity of $143 \, \frac{m}{s}$, outside from transonic effects. The DEP propellers develop an overall $P_b = 420 \, kW$ and further will be defined with a diameter of $0.80 \, m$ and operating at $3400 \, RPM$ (tip velocity of $143 \, \frac{m}{s}$).

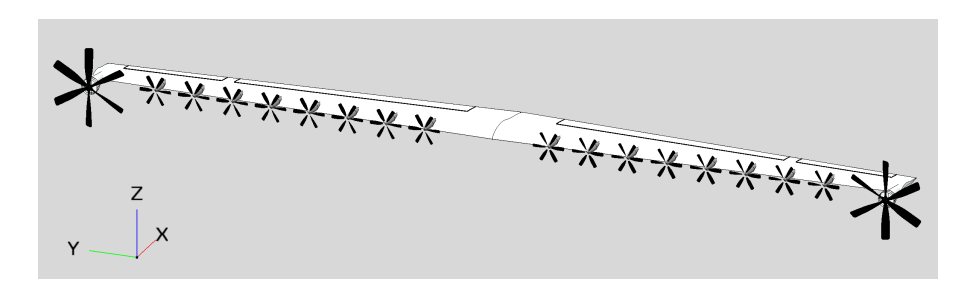


Figure 4 – Representation of ZETHA wing, with cruise propellers and DEP.

More in-depth analyses have been conducted to provide a preliminary estimate of the aircraft's structural masses. Initially, weight estimation has been based on statistically derived formulas, as the ones provided by Sadraey [5]. Subsequently a further more detailed and structured weight estimation has been performed due to the unconventional typology of the aircraft: ZETHA poses challenges for weight comparison due to distinct propulsion and battery systems, to the high aspect ratio wing with multiple distributed propellers and motors, and since the cruise propellers are installed at wingtips,

demanding careful structural and aeroelastic considerations. The structural sizing has been done in *NeoCASS* through sizing loads based on certification rules (EASA CS23).

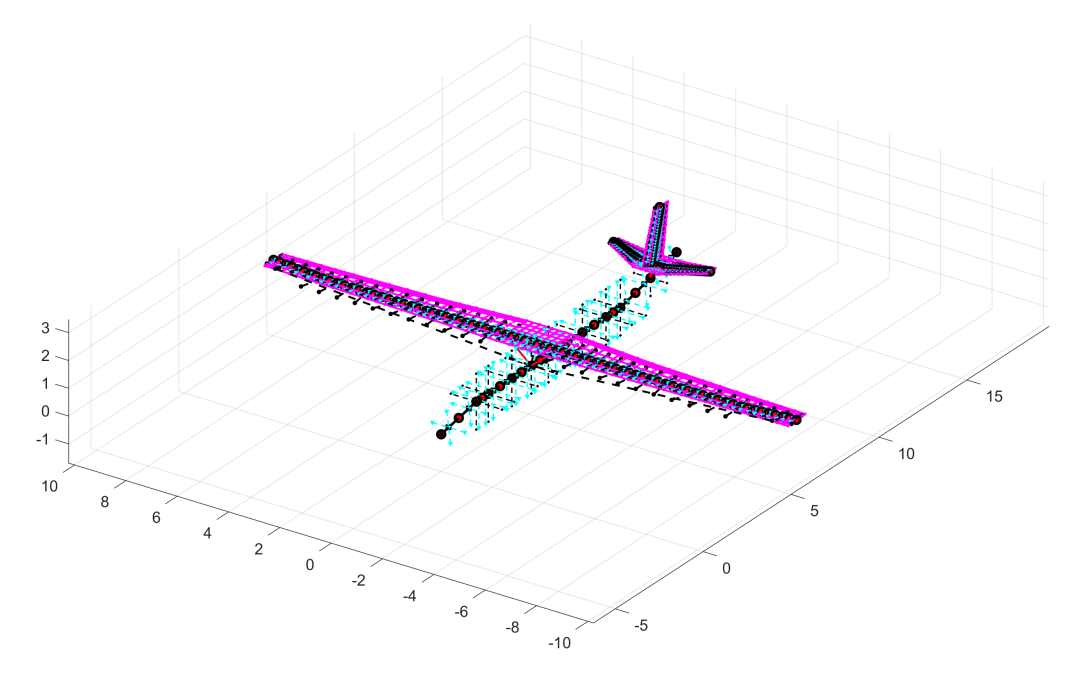


Figure 5 – FEM model implemented in NeoCASS.

The main challenges encountered have been to implement the DEP propellers and the battery packs, since not specifically included. Relatively, an extension of the code to dispose additional masses and the design of boxes with the correct density have solved the problems. The outcome of the investigation has revealed a similar overall total weight, but a different weight distribution, which affects the stability of the aircraft. The static (static margin $S.M. \simeq 8\%$) and dynamic stability have been calculated from the data retrieved by the mass estimation and the updates models designed in OpenVSP and XFLR5.

The design yields to the following geometrical results.

Component	S	b	D_{max}
Wing	$27.40 m^2$	20.8 m	-
H. Tail	$3.56 m^2$	3.8 m	-
V. Tail	$1.83 m^2$	1.6 <i>m</i>	-
Fuselage	$72.48 m^2$	-	2m

Table 2 – ZETHA geometry.

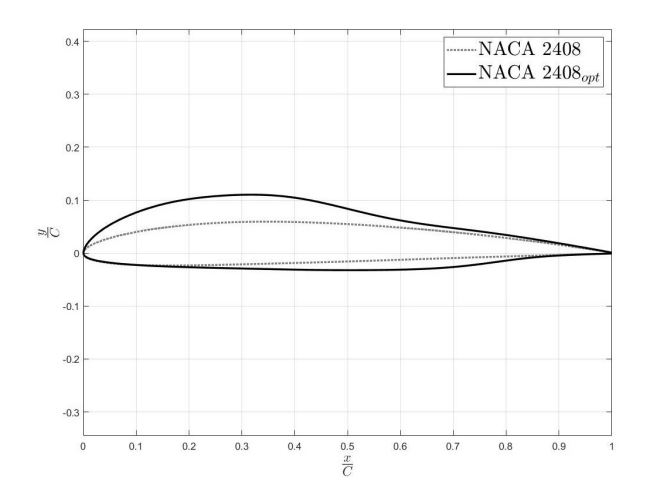
3. 2D Aerodynamic Optimization

The first step of aerodynamic investigation consists in selecting the optimal airfoil, ensuring the required performance for the design phase and maximizing efficiency. Additionally, the study involved examining high-lift capabilities of the airfoil through the design of a Fowler flap. A CFD analysis at high angles of attack has been performed on the airfoil with the flap deployed.

3.1 Airfoil Optimization

The airfoil optimization process began by considering a range of profiles with performance close to those required by the Preliminary Design and significant thicknesses capable of accommodating the propulsion subsystems for DEP and the wing structure. The airfoils used in the optimizations are the following: NACA 2408, GOE 623, EPPLER 854, NACA 63212. Consequently, multiple multi-objective optimizations were conducted in *Xoptfoil* for each airfoil, defining and assigning weights to objective parameters for optimization across different flight conditions and imposing geometric constraints on

various optimizations. Greater weight was placed on optimizing the lift-to-drag ratio during cruise, maximizing $C_{L\,max}$ during landing, and minimizing C_m during cruise in terms of importance for weight. The optimization process adopted consists in both global and local searches: first, a particle swarm optimization used as the global search method, then, a simplex method for the local search. The choice of the airfoil has been made after a comparison and the definition of a scoring system. It is important to tend to the right compromise between a high C_L , a high cruise lift to drag ratio $\left(\frac{L}{D}\right)_{cruise}$, which is directly related to the range of the aircraft, and a low C_m of the wing. Moreover, it has been paid attention at maximizing F, defined as $F = E\sqrt{C_L}$ which primarily impacts the climb phase. The best results of the optimization process correspond to those obtained for the optimized airfoil 2408_{opt} , represented here geometrically and in terms of performance (figures 6, 7 and table 3).



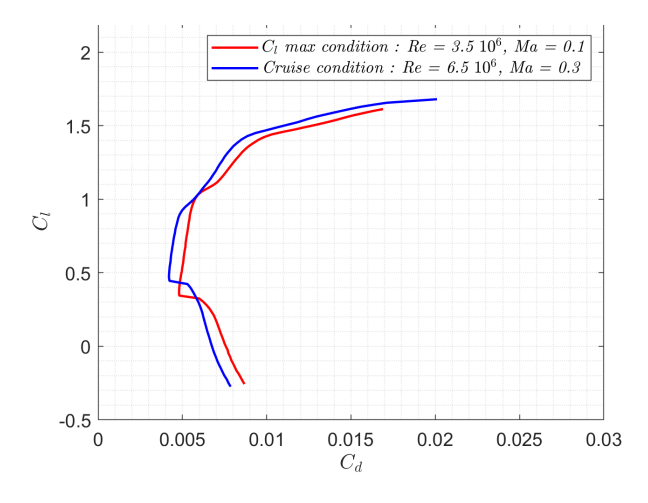


Figure 6 – 2408_{opt} representation.

Figure 7 – C_l – C_d plot for the 2408_{opt} .

$\frac{t}{c}$	E_{cruise}	C _{l max clean}	C_{l0}
14%	123	1.53	0.53
$C_{d min}$	C _{m cruise}	$C_{l\ Emax} - C_{l\ cruise}$	F_{max}
0.0041	-0.0408	0.396	198

Table $3 - 2408_{opt}$ performance.

3.2 Flap Design

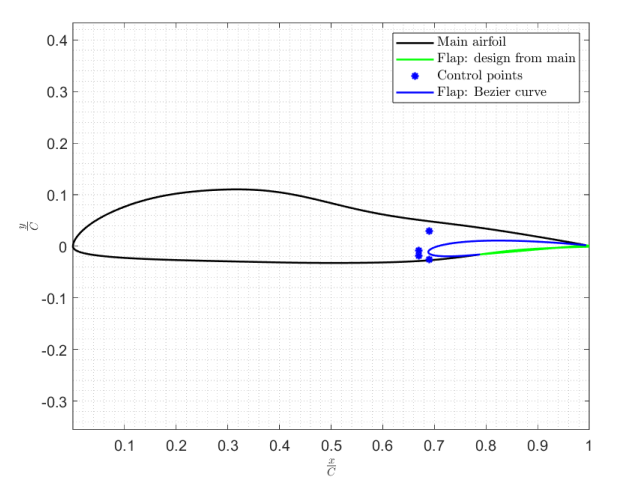


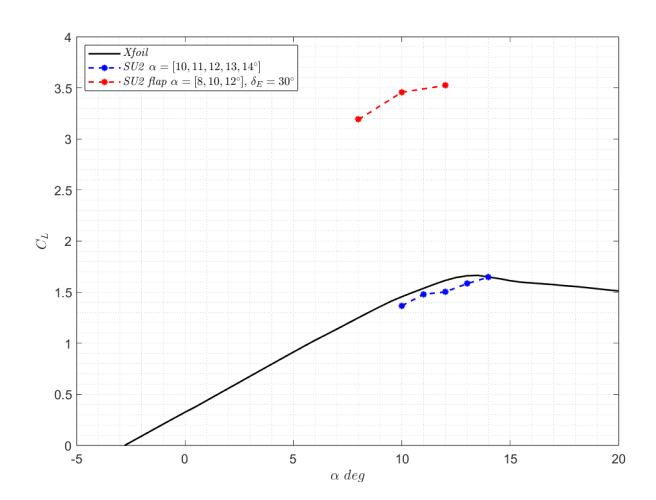
Figure 8 - Flap design.

In sight of being able to investigate the high-lift capabilities of the wing, a further study has been done on the airfoil, through the design and the CFD analysis of a flapped configuration. A Fowler flap has been created in *MATLAB* (figure 8).

In order to design smooth fitting between the 2408_{opt} and the flap, in the region where the flap requires to be extracted, Bezier curves have been used. The CFD analyses have been performed on SU^2 with a 275000 elements mesh, after having assured grid convergence, on both the clean airfoil and the flapped airfoil in landing condition, from 10° to 14° . In this way the 2408_{opt} polar obtained through Xfoil has been compared to the CFD results to get more reliable outcomes and the high-lift capabilities have been assessed.

	C_l	$C_{l flap}$	Lift increment
$\alpha = 12$	1.50	3.52	135%

Table 4 – Lift coefficient increment due to flap deployment, data from CFD 2D.



- 6.3e+01 - 62 - 61 - 60 - 60 - 59 - 58e+01

Figure 10 – Pressure visualization at 12°.

Figure $9 - C_l - \alpha$, Re = 3500000, Ma = 0.1.

4. 3D Aerodynamic Analyses

In the present Section the propulsive aerodynamic enhancements due to DEP, expected to increment the C_L of about 20-30% with wing clean configuration and at a levelled angle of attack, are analyzed to retrieve the ultimate $C_{L\,max}$ of ZETHA.

Due to the limited computational power available, the problem has been faced from different point of views, adopting empiric considerations on the wing aerodynamic performance.

The various analyses that have been presented are as follows: a first low-fidelity VLM parametric analysis using VSPAERO to establish the C_L increase at different angles of attack due to DEP system activation (modeled with actuator disk, AD), and a more accurate investigation using a panel method solver in DUST, on a limited section of the wing interacting with a single DEP propeller. The actual aim is to analyze the ideal configuration of DEP propellers in order to maximize the beneficial effects in terms of increasing the C_L . The interaction of the propeller slipstream with the wing is well described by Veldhuis [4] and is characterized by two main effects. The first is an increase in axial velocity, which leads to a corresponding increase in dynamic pressure seen by the wing, characterized by a symmetric velocity distribution relative to the center of the propeller. The second effect involves a velocity induction due to the propeller swirl, thus characterized by an antisymmetric velocity distribution. In light of these considerations a study has been conducted to investigate the variation of three main parameters of a single DEP propeller to retrieve the maximum wing section C_L enhancement: the diameter (D_p) , the vertical position normalized to the propeller radius (z_p/D_p) , and the longitudinal one relative to the leading edge of the wing $(-x_p/D_p)$. The variation in D_p/MAC naturally results in the change of the number of propellers implemented in the DEP system.

D_p/MAC	z_p/D_p	$-x_p/D_p$
{0.4,0.55,0.7}	$\{-0.2, 0, 0.2\}$	[0.2, 0.7]

Table 5 – Geometrical propeller's parameters variations.

4.1 VLM and AD

As mentioned, the first analysis performed is the one done with the VLM and AD, aimed at highlighting the trend of lift enhancement, varying the number of DEP propellers only. The required quantities to define the modeling of the AD are the thrust and power coefficients, C_T and C_P , and the rotational speed of the propeller, RPM. The Renard formulas presented below have been used to determine these quantities both for the DEP and the cruise propellers, setting a reasonable propeller efficiency $\eta_{prop} = 0.75$, considering therefore variable pitch propellers in particular for the cruise ones.

$$\begin{cases} \eta_{prop} = \frac{JC_T}{C_P} = 0.75 \\ C_P = \frac{\frac{P_b}{n_{DEP}}}{\rho_{cruise}(\frac{RPM}{60})^3 D_p^5} \\ C_T = \frac{\frac{T}{n_{DEP}}}{\rho_{cruise}(\frac{RPM}{60})^2 D_p^4} = \frac{\frac{P_b \cdot \eta_{prop}}{\nu \cdot n_{DEP}}}{\rho_{cruise}(\frac{RPM}{60})^2 D_p^4} \end{cases}$$
(3)

The analysis reveals that increasing the number of DEP propellers, and consequently, the distribution of the total DEP power ($420\,kW$) among them, leads to a substantial advantage in aerodynamic performance, up to 40% of enhancement in a take-off or landing condition with $\alpha=0^{\circ}$.

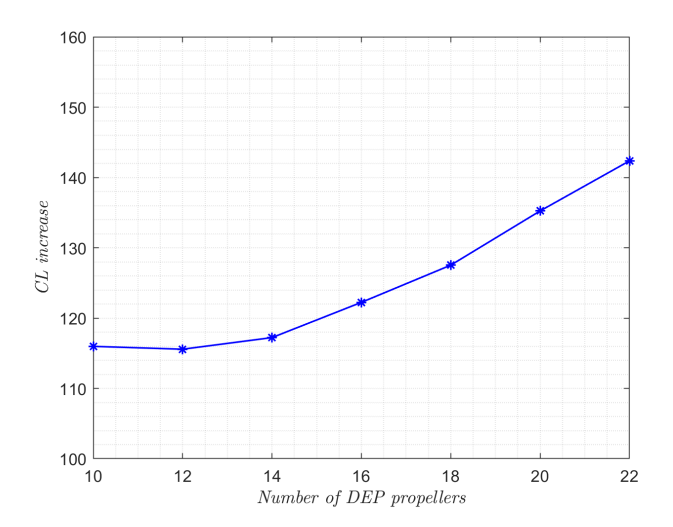


Figure $11 - 2408_{opt}$ representation.

However, one must consider the limitations of the models: indeed, the wing is modeled without accounting for thickness, which can have significant effects, and the AD is a simplified 1D model of the propeller. The following table shows the parameters variation for the propellers chosen to be investigated also in the next analyses with the panel method in order to guarantee the power required by the DEP.

Other investigations have been performed with VLM and AD, especially a set of analyses concerning the high-lift setup, with DEP activated, with $\delta_{Flap}=30^{\circ}$ and $\delta_{Aileron}=10^{\circ}$, which at $\alpha=12^{\circ}$ retrieved a $C_{L\,max}=2.833$ for $Setup\ A$ and $C_{L\,max}=2.799$ for $Setup\ B$. The DEP Setups analyzed have been chosen since they are the most likely to be used, with respect to the $Setup\ C$.

	$D_p[m]$	n	C_T	C_P	RPM
Setup A	0.6	22	0.44	0.46	4550
Setup B	8.0	16	0.34	0.36	3414
Setup C	1.0	12	0.29	0.30	2730

Table 6 – Propellers parameters.

4.2 Panel Method

The mid-fidelity analysis consists in simulating a system composed of a wing section and a single propeller, varying the characteristic parameters from case to case, describing the wing section using a panel method and the propeller blades as lifting lines, abandoning the AD. The advantages of this more reliable model is that the wing thickness is accounted for and the propeller is simulated in an unsteady fashion. Moreover the wake-surface problematic interaction for panel methods is solved by modeling the wake with vortex elements. However, this is a computationally more demanding method, making sensitivity analysis on the entire wing with DEP unfeasible. Therefore, the test case used considers a wing section of chord corresponding to the mean aerodynamic chord (MAC) and a span of 3 m. The simulations are run at take-off or landing conditions, with a proper wing discretization (70 elements in both chord and span), more dense along the leading edge, with a timestep of 1/40 propeller revolution time (considering the intermediate propeller diameter case), and 8 total revolutions in order to get the C_L averaged on the last revolution being different no more than 1% to the one averaged on the second-to-last rotation. All achievable combinations by varying the parameters D_p , z_p/D_p , $-x_p/D_p$ were simulated to achieve the configuration that yielded the highest C_L of the wing section compared to the case of the wing section without propellers. The results (figure 12) were considered by referring to scaled values $(\frac{\Delta C_L}{P})$ relative to the shaft power of the different propellers, ensuring that interference with the wing did not degrade the C_T value, particularly for Setup A since it has a smaller D_p .

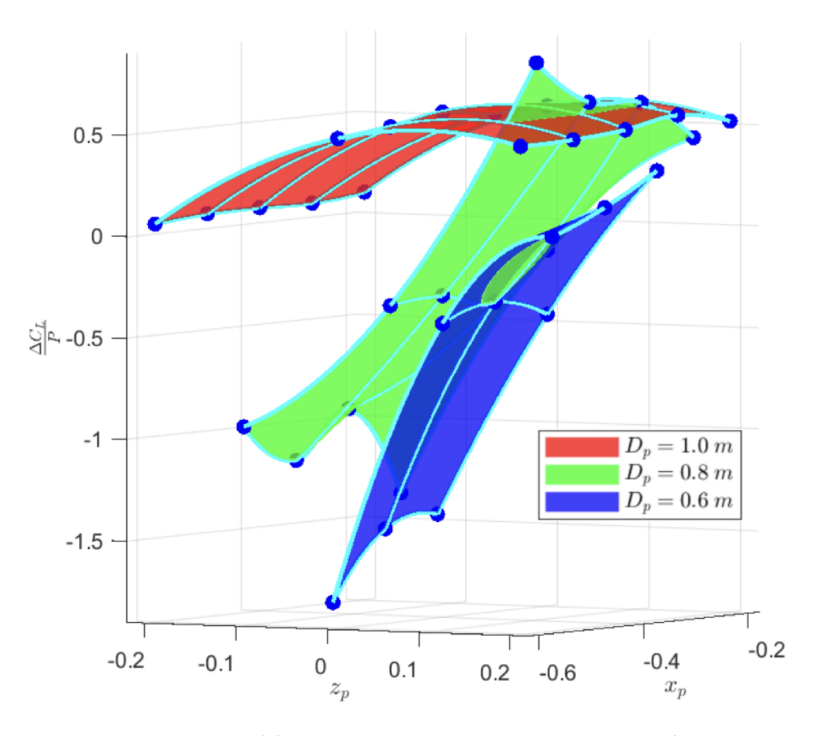


Figure 12 – $\frac{\Delta C_L}{P}$ for the different propellers, $\left[\frac{1}{kW}\right]$.

From the results, it emerges that the wing thickness produces significant effects, especially in cases with small D_p (e.g. $Setup\ A$), making this investigation crucial. It is noticeable that, as expected from theory, the vertical displacement $\frac{z_p}{D_p}$ of the propeller is the most sensitive parameter to variations: for all $Setups\ A$, B, C, the case with $\frac{z_p}{D_p}=0.2$ yields the best lift enhancement. The parameter of

longitudinal displacement $\frac{-x_p}{D_p}$ is not always particularly impactful, except in *Setup B*, where the performance in the case $\frac{z_p}{D_p}=0.2$ increases with the distance from the leading edge, presumably due to the contraction of the slipstream. The preferred configuration identified is *Setup B*, with $\frac{z_p}{D_p}=0.2$, $-x_p=0.5\,m$ resulting in a $\Delta C_L=23.2\%$ for the wing section, with C_T almost unchanged.

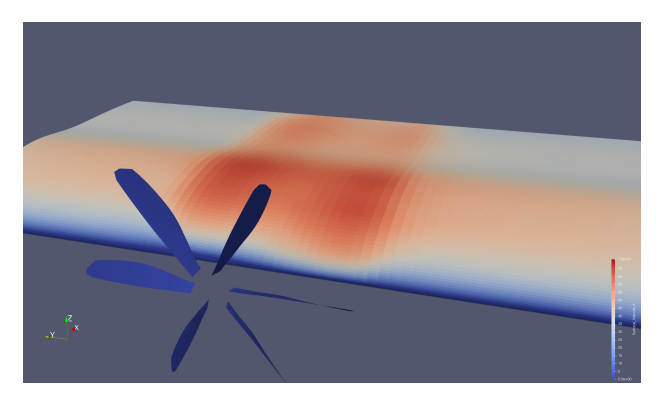


Figure 13 – Surface velocity in x direction representation, Setup B.

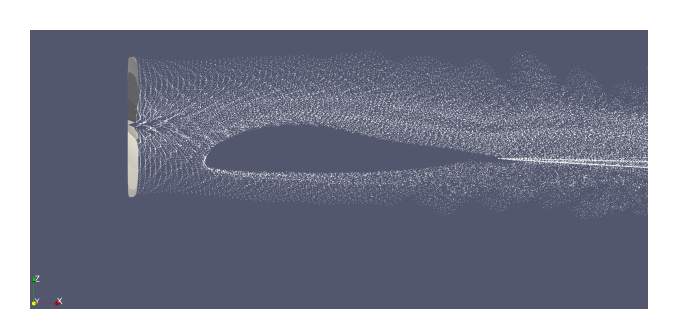


Figure 14 – Flow representation for Setup B.

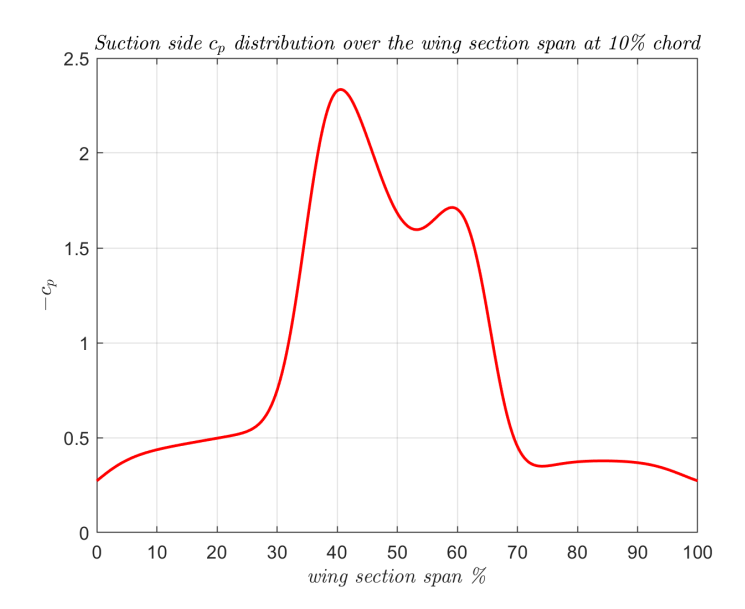


Figure $15 - C_p$ distribution on the suction side of the wing section span analyzed, at 10% of the chord.

5. Conclusions

The preliminary design of a fully electric thin-haul aircraft, ZETHA, has been presented. It accommodates 7 passengers along with 2 pilots and their respective luggage, offering a maximum range of $400\,km$ in less than 80 minutes. ZETHA is an innovative concept of aircraft that embodies environmental sustainability and efficiency while ensuring a significant operational range. The introduction of Distributed Electric Propulsion (DEP) technology has been assessed and investigated to attain aerodynamic improvements through electric propulsion. The results demonstrate that deploying smaller motors and consequently smaller propellers across the wing span yields enhanced aerodynamic performance, leading to substantial benefits. The analyses yielded the most efficient DEP configuration in terms of ΔC_L . Through further comparisons with the VLM, which for the same case on the wing section identifies a ΔC_L 15% higher, it is deduced that the increase in C_L for the entire wing under take-off conditions at $\alpha=0^\circ$ is approximately 20-25% of the clean wing lift coefficient, as initially anticipated. This value could rise, making the DEP even more effective in the case of deployed flaps and high angles of incidence, where the slipstream generated by the propellers could hinder flow

separation. This case has been simulated with VLM and AD and, with a plain flap less effective than the Fowler one designed, $C_{L\,max}=2.799$ is obtained, which is an optimistic estimate of the maximum attainable C_L .

However, it's improbable that the maximum attainable value will fall below the $C_{L\,max}$ specified by the design ($C_{L\,max\,LND}=2.31$). Instead, it is anticipated to surpass it significantly.

To obtain precise values under such conditions, it is beneficial to resort to high-fidelity methods (CFD) capable of assessing the entire wing with active DEP and the interactions among the propellers themselves. The enhancement of performance, therefore, can lead to significant modifications in the conceptual design of the aircraft:

- definition of a higher wing loading with respect to the designed one, leading to a reduction of wing surface and therefore of friction drag, due to the enhancement in $C_{L\,max}$ during high-lift phases as take-off and landing due to DEP;
- change in the flap type (e.g. plain flap);
- reduction of the flap surface or even contemplating not implementing the high-lift surfaces;
- modification of the optimization goals used to define the airfoil in favor of greater efficiency during the cruise phase.

Many other developments could be assessed:

- 1. better design of the DEP propellers' pods in order to minimize the reduction in operational range due to their drag, which is preliminary esteemed to be 15 km over the design route of 400 km;
- 2. three-dimensional CFD analysis of the flaps effect with and without activated DEP, to obtain reliable values of aerodynamic performance even at high angles of attack;
- 3. stall progression analysis, evaluating the application of wing twist or considering the use of different airfoils along the span in order to anticipate stall at the wing root rather than at the tip.

6. Contact Author Email Address

mailto: giacomo.beghetto@gmail.com mailto: maurizio.boffadossi@polimi.it

7. Copyright Statement

The authors confirm that they, and/or their company or organization, hold copyright on all of the original material included in this paper. The authors also confirm that they have obtained permission, from the copyright holder of any third party material included in this paper, to publish it as part of their paper. The authors confirm that they give permission, or have obtained permission from the copyright holder of this paper, for the publication and distribution of this paper as part of the ICAS proceedings or as individual off-prints from the proceedings.

References

- [1] Anusha Harish, Perron Christian, Bavaro Daniel, Ahuja Jai, Ozcan Melek, Justin Cedric Y, Briceno Simon I, German Brian J, and Mavris Dimitri. Economics of advanced thin-haul concepts and operations. In 16th AIAA Aviation Technology, Integration, and Operations Conference, page 3767, 2016.
- [2] Roskam Jan. Airplane Design. University of Kansas, 1st edition, 1997.
- [3] Bugga Kumar, Jones John-Paul, Jones Simon, Krause Charlie, and Pasalic Jasmina. Performance assessment of prototype lithium-sulfur cells from oxis energy. *Jet Propulsion Laboratory, National Aeronautics and Space Administration NASA*, 2018.
- [4] Veldhuis L L. *Propeller Wing Aerodynamic Interference*. PhD thesis, Faculty of Aerospace Engineering, Delft University of Technology, Delft, The Netherlands, 2005.

- [5] Sadraey M. *Aircraft Design: A systems engineering approach*. Daniel Webster College, New Hampshire, USA, 2013.
- [6] Della Vecchia Pierluigi, Malgieri Daniele, Nicolosi Fabrizio, and De Marco Agostino. Numerical analysis of propeller effects on wing aerodynamic: tip mounted and distributed propulsion. *Transportation research procedia*, 29:106–115, 2018.
- [7] Zhao Tianyuan. Propulsive battery packs sizing for aviation applications. *Embry-Riddle Aeronautical University*, 2018.